Magnetic cloud boundary layer of 9 November 2004 and its associated space weather effects

P. B. Zuo,[1,2] F. S. Wei,[1] X. S. Feng,[1] X. J. Xu,[1,3] and W. B. Song[1]

Received 21 August 2009; revised 12 March 2010; accepted 26 March 2010; published 2 October 2010.

[1] On 9 November 2004, the WIND spacecraft detected a magnetic cloud boundary layer (MCBL) during the interval from 19:07 UT to 20:30 UT. Within the MCBL, there is intense southward magnetic field and the dynamic pressure is rather high, which makes it much geoeffective. Twenty-three minutes later, the MCBL arrived on the magnetopause. An intense geomagnetic storm main phase was driven by the sustaining strong southward magnetic field within the MCBL. During the passage of the MCBL, a typical magnetospheric substorm was triggered. The substorm onset was synthetically identified by the aurora breakup, magnetic dipolarization, dispersionless particle injection, Pi2 pulsation, and the polar bay onset. The substorm triggering is related to the special magnetic and plasma structure within the MCBL. The MCBL accompanying adjacent sheath region formed a dynamic pressure enhancement region, which strongly compressed the magnetosphere and even pushed the magnetopause into the geosynchronous orbit so that two dayside spacecraft GOES-10 and GOES-12 were directly exposed in the magnetosheath for a long interval during the passage of the MCBL. In terms of *Shue et al.* (1998) model, the closest subsolar standoff distance even reached 5.1 R_E during the passage of the MCBL. It can be inferred that the strong dynamic pressure and the strong discontinuities within the MCBL determine the intense compression effect. In addition, a very intense geomagnetically induced current (GIC) event was directly caused by the MCBL. Similar to this case, majority of MCBLs are dynamic pressure enhancement regions, and there are strong southward magnetic field and several strong discontinuities inside these regions, which can potentially drive large-scale magnetospheric activities. In this paper, we take a case study to discuss the magnetospheric activities and the space weather effects caused by MCBLs.

Citation: Zuo, P. B., F. S. Wei, X. S. Feng, X. J. Xu, and W. B. Song (2010), Magnetic cloud boundary layer of 9 November 2004 and its associated space weather effects, *J. Geophys. Res.*, *115*, A10102, doi:10.1029/2009JA014815.

1. Introduction

[2] The magnetic clouds (MCs) are common transients in the solar wind and usually regarded as one of the interplanetary manifestations of coronal mass ejections (CMEs) characterized by enhanced magnetic field, low proton temperature and plasma β, and smooth rotation in the magnetic field [*Burlaga*, 1995]. Although many aspects related to MCs are much clear now, there are still many topics left unsolved. How to identify the boundaries of the MC is one of such problems that is urgent to be investigated because it is related to many important issues like the reconstruction of the magnetic cloud and the interaction between the solar wind and the MC [*Burlaga*, 1995; *Wei et al.*, 2003a]. Based on statistical analysis on the boundary characteristics of 80 MCs detected in 1969–2001, *Wei et al.* [2003a] first proposed that the boundary of the MC is not a simple boundary separating the MC from the solar wind (SW) but a complex boundary layer with internal temporal and spatial structures, and named these structures front and tail magnetic cloud boundary layers (MCBLs), respectively. The front MCBL is formed due to the interaction between the magnetic cloud and front slow solar wind when the MC propagates in interplanetary space. For some MCs followed by fast flows or shocks, tail MCBL is possibly formed [*Wei et al.*, 2003a]. The MCBLs are characterized by the obvious magnetic signatures including the magnetic decrease inside the boundary layer like magnetic holes, the magnetic field azimuthal angle and the latitudinal angle change ($\Delta\phi \sim 180°$, $\Delta\theta \sim 90°$) near the center of MCBLs, as well as the corresponding plasma features (relatively high proton temperature, high plasma β, high proton density, and as a result high dynamic pressure) [*Wei et al.*, 2003a, 2003b, 2006]. In addition, majority of MCBLs are bounded by directional

[1]SIGMA Weather Group, Center for Space Science and Applied Research, State Key Laboratory of Space Weather, Chinese Academy of Sciences, Beijing, China.
[2]Department of Physics and Space Sciences, Florida Institute of Technology, Melbourne, Florida, USA.
[3]Graduate University of Chinese Academy of Sciences, Beijing, China.

0148-0227/10/2009JA014815

discontinuities. The MCBL is often a non-pressure-balanced structure with obvious decrease of the magnetic pressure inside which the total pressure (the sum of thermal pressure and magnetic pressure) is usually lower than that in the solar wind and magnetic cloud body [*Wei et al.*, 2006]. These results show that there exist important dynamic processes inside MCBLs.

[3] The solar wind, magnetosphere, and ionosphere form a complicated coupling system [*Lyon*, 2000]. When the solar wind impinges on the magnetopause, part of plasma, momentum and energy are transported from the solar wind into the magnetosphere. In a quiescent situation, energy flow is gradual and the energy transported from the solar wind is dissipated in the ionosphere or magnetospheric ring current region or deposited in the magnetotail. On the other hand, when the multiple-scale disturbance structures interact with the magnetosphere, the electric field and current systems in the magnetosphere and ionosphere are notably changed, and the near-Earth radiation is also obviously enhanced. On some extreme conditions, the deposited energy is abruptly released and it consequently triggers the geomagnetic storm, magnetospheric substorm, or other large-scale magnetospheric activities. Such physical phenomena may affect or seriously destroy the current space-based and ground-based technical systems. Thus it is of application value to make clear the relationship between the disturbances in the solar wind and geomagnetic activities from the viewpoint of space weather. Actually the study on this issue is mainly emphasized on two aspects: the magnetospheric responses to special structures in the solar wind, such as the corotating streams, interplanetary shocks, magnetic clouds, corotating interaction regions [e.g., *Huttunen and Koskinen*, 2004; *Schwenn*, 2006], as well as the interplanetary sources of large-scale magnetospheric activities such as storm, substorm, magnetospheric steady convection, etc. [e.g., *Akasofu*, 2004; *Borovsky and Denton*, 2006; *Pulkkinen*, 2007; *Sergeev et al.*, 1996].

[4] The MCBL is an important meso- and small-scale structure in the solar wind with timescale of a half hour to a few hours. So far, it has not yet been intensively investigated about the magnetospheric responses during the passage of MCBLs [*Zuo et al.*, 2007]. It has been suggested that interplanetary magnetic field B_z component and the solar wind dynamic pressure are two most important parameters in controlling geomagnetic activities and affecting the coupling of the solar wind and the magnetosphere [*Lyon*, 2000; *Pulkkinen*, 2007]. *Zuo et al.* [2007] statistically analyzed the characteristics of the magnetic field B_z component (in GSM coordinates) inside MCBLs based on 35 typical MCBLs observed by WIND in 1995–2006. It is found that the magnetic field B_z polarity inside the BLs have three states: entirely southward ("S" type), entirely northward ("N" type), bipolar (the polarity changes at least for one time or B_z fluctuates around zero point, named "F" type). Majority of MCBLs (91%) belong to "F" type [*Zuo et al.*, 2007]. Many discontinuities can be found inside MCBLs. Furthermore, as we studied, the dynamic pressure inside nearly all MCBLs is far larger than that in the magnetic cloud body and the adjacent sheath region with the value of 2–40 nPa, whereas usually the dynamic pressure in the magnetic cloud is lower than 2 nPa. For some events, the dynamic pressure in the sheath region near the MCBL is also high, so the MCBL accompanying the adjacent sheath region forms a dynamic pressure enhancement region. And for a majority of events, the MCBL is an isolated dynamic pressure enhancement region. The front and tail boundary of MCBL is commonly rapid, strong dynamic pressure pulse (DPP) corresponding to the abrupt change in plasma density and special structure such as directional discontinuity, fast shock, slow shock, or magnetic decrease region [*Zuo and Feng*, 2007; *Zuo et al.*, 2006]. Considering the special magnetic and plasma features of MCBLs, it is intriguing to investigate the magnetospheric responses and space weather effects when the MCBLs cross the magnetopause.

[5] In this paper, the global magnetospheric responses to the passage of MCBLs are investigated by case study. The magnetic cloud boundary layer discussed was detected by WIND on 9 November 2004. In section 2, we describe the magnetic and plasma characteristics of this MCBL and the magnetic cloud. Although the radial scale of this MCBL is rather small, it directly drove an intense magnetic storm and triggered a typical substorm that occurred in the expansion phase of the storm. We perform a thorough analysis of the substorm activities based on the data from several spacecraft including POLAR, LANL, and TC-1 as well as the geomagnetic field data. Furthermore, the geosynchronous spacecraft GOES-10 and GOES-12 were right on the dayside and crossed the magnetopause many times. In terms of the GOES observations and the empirical magnetopause model of *Shue et al.* [1998], the compression effect of the MCBL on the Magnetosphere is also investigated. Associated with geomagnetic variations, geomagnetically induced current (GIC) may flow in the power grids and pipelines. For this MCBL, a very large GIC event is directly driven. We discussed the GIC observations from Finnish natural gas pipeline. Above space weather effects during the passage of this MCBL are analyzed in detail in section 3. In section 4 we present the summary.

2. Magnetic Cloud Boundary Layer

[6] Figure 1 presents the magnetic field data from WIND/MFI and plasma data from WIND/SWE (Figure 1a) and 3DP (Figure 1b) on 9–10 November when WIND was located at $\mathbf{r} = (200, 50, -35)\ R_E$ (in GSM). The panels from top to bottom are intensity, latitudinal angle, longitudinal angle, and B_z component of the magnetic field, plasma bulk velocity, proton temperature, number density, and the solar wind dynamic pressure, respectively. During the interval between 20:30 UT on 9 November and 16:36 UT on 10 November, WIND observed a typical magnetic cloud (see the region between two vertical lines labeled by "G_f" and "G_t" in Figure 1b). The magnetic cloud is identified based on several magnetic field and plasma signatures including strong magnetic field with a maximum of 42.7 nT, smooth rotation in the direction of magnetic field (see the θ and ϕ panels), exceptionally low proton temperature. It is a fast magnetic cloud with maximum velocity of 800 km/s, and inside the magnetic cloud the solar wind dynamic pressure is rather higher relative to usual magnetic clouds. This magnetic cloud is associated with two leading shocks, which are detected by WIND at 09:19 UT and 18:25 UT on 9 November (labeled by "S_1" and "S_2," respectively, in Figure 1). Across the shock front, the magnitude of the magnetic field is notably

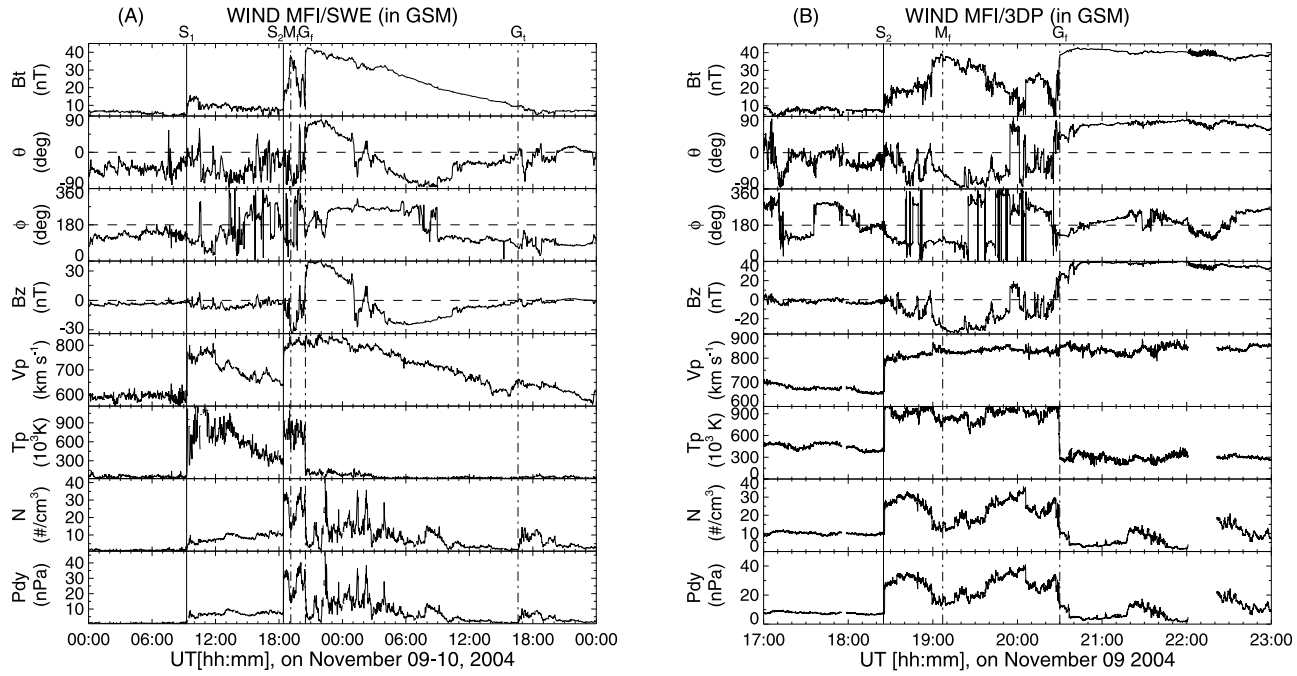

Figure 1. Plot of the magnetic field and plasma data from WIND on 9–10 November 2004 to present the structure of the magnetic cloud and the magnetic cloud boundary layer.

enhanced, and the proton temperature, number density, and plasma bulk velocity also increase.

[7] The magnetic cloud boundary layer formed between the shocked solar wind (that usually named as sheath region) and the magnetic cloud body was observed by WIND during the interval of 19:07–20:30 UT (labeled by "M_f" –"G_f" in Figure 1). Figure 1b gives the high-resolution magnetic field and plasma data to show the fine structure of the magnetic cloud boundary layer. The characteristics of this MCBL are as follows. (1) There is strong sustaining southward magnetic field inside the MCBL, and inside the adjacent cloud body the magnetic field is northward. (2) The MCBL accompanying the adjacent sheath region form a dynamic pressure enhancement region with averaged dynamic pressure of 30 nPa, which is attributed to the relative high number density. It is expected that the magnetosphere is strongly compressed by this dynamic pressure enhancement region.

3. Space Weather Effects of the Magnetic Cloud Boundary Layer

[8] At 18:48 UT, a sudden impulse (SI) in geomagnetic field was induced by the shock "S_2" due to the compression of the strong dynamic pressure pulse in the postshock region. Therefore, it can be inferred that the transit time for the shock "S_2" from the WIND spacecraft to the magnetopause is 23 min if the response time of the magnetosphere to the shock is not considered, which can be reasonably neglected. Furthermore, provided it takes the MCBL and the driven shock the same time to propagate from WIND to the magnetopause, the transit time for the MCBL is also 23 min. So the MCBL interacted with the magnetosphere from 19:30 through 20:53 UT.

3.1. Compression Effect of the MCBL on the Magnetosphere

[9] *Shue et al.* [1998] model is an excellent magnetopause model that has been applied to space weather prediction. In this model the shape and position of the magnetopause are dependent on two parameters: the solar wind dynamic pressure P_{dy} and IMF B_z component. This model can also be applied in extreme solar wind condition with strong dynamic pressure and sustaining strong southward magnetic field. Figure 2a presents the shifted WIND data including interplanetary magnetic field intensity and B_z component (in GSM) and solar wind dynamic pressure, as well as the calculated subsolar standoff distance r_0 in terms of *Shue et al.* [1998] model (WIND data has been shifted by 23 min, i.e., the transit time for the MCBL propagating from WIND to the magnetopause). It can be seen that when the dynamic pressure enhancement region composed of the sheath region and the MCBL compressed the magnetosphere, the magnetopause was intensively pushed into the geostationary orbit ($r_0 < 6.6R_E$).

[10] When the MCBL and the front adjacent sheath region crossed the magnetosphere, GOES-10 was located at the MLT of 09:59–11:57, and GOES-12 was located at the MLT of 14:00–15:58, i.e., both spacecraft were near the noon and distributed on two sides of the noon. The GOES observations can identify the magnetopause crossings. Figures 2c and 2d show the responses of the magnetic field observed by GOES-10 and GOES-12 when the MCBL crossed the magnetosphere. The B_z component was negative for most time during the passage of the MCBL and adjacent sheath region, and the change tendency of B_z was similar to that inside the MCBL when B_z was negative, but B_z observed by GOES was much larger than that inside the MCBL observed by WIND. It is known that B_z at geosynchronous orbit is

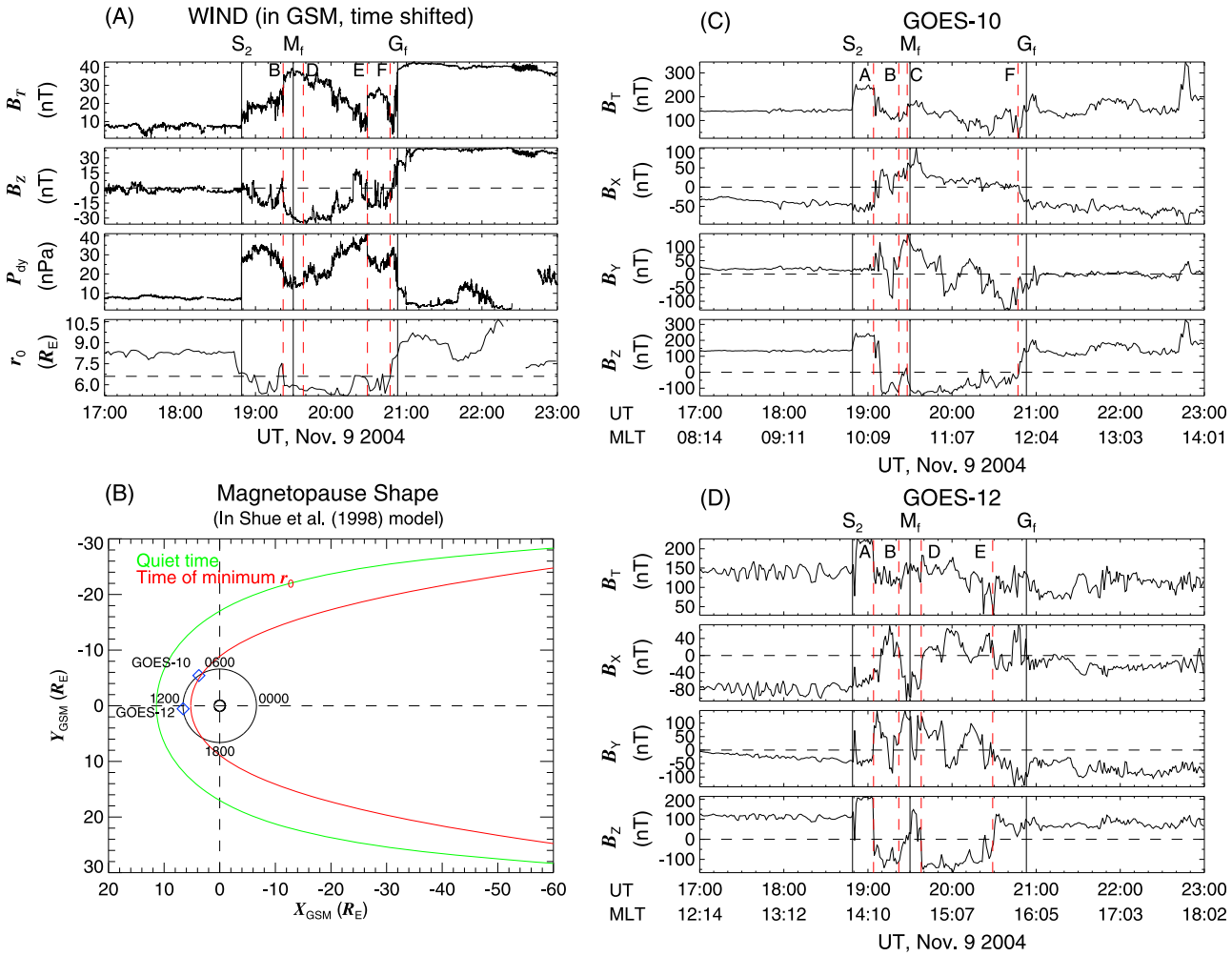

Figure 2. Intense compression to the magnetosphere of the magnetic cloud boundary layer in terms of GOES magnetic field data and *Shue et al.* [1998] model. (a) The solar wind data observed by WIND that are shifted by 23 min. (b) The shapes of the magnetopause in terms of *Shue et al.* [1998] model when in the quiet solar wind and when the subsolar is closest to the Earth during the passage of MCBL; (c) GOES-10 observations; (d) GOES-12 observations.

always northward in quiet solar wind when GOES is located in the magnetosphere since the magnetic field is near dipolar on this condition. So it is concluded that GOES-10 and GOES-12 were not in the magnetosphere when the spacecraft observed the negative magnetic field. The MCBL and adjacent sheath region form a dynamic pressure enhancement region compared with background solar wind and the magnetic cloud body. The magnetopause was strongly compressed by the dynamic pressure enhancement region and even pushed into the geosynchronous orbit, so that the two GOES spacecraft crossed the magnetopause and were in the magnetosheath for a long interval. Therefore the two spacecraft detected the compressed magnetic field in the magnetosheath which has similar change form to that observed by WIND in the solar wind. The phenomena that the magnetopause enters into the geosynchronous orbit are much rare and often occur on extreme solar wind conditions. The exceptional strong dynamic pressure in the MCBL forms the extreme solar wind conditions. As we know, there are many spacecraft distributing at the geosynchronous orbit. If the magnetopause is pushed into the geosynchronous orbit, some of the dayside spacecraft will be directly exposed to the magnetosheath magnetic field, solar energetic particle and cosmic ray, that perhaps does harm to the spacecraft or the payloads.

[11] It can be seen from GOES-10 observations (see Figure 2c) that there are four magnetopause crossings denoted by the vertical lines labeled by "A," "B," "C." and "F" respectively. The criteria to determine that the spacecraft is in the magnetosheath are that the observed magnetic field B_z component is negative and its change tendency is similar to that of the solar wind. In the region between two vertical lines labeled by "A" and "B" and in the region between "C" and 'F," GOES-10 was located in the magnetosheath due to the compression of the MCBL. At 19:04 UT, the magnetopause was strongly compressed and pushed earthward so as to be crossed by GOES-10 at the geosynchronous orbit; at 19:21 UT, the magnetopause moved sunward and was crossed by GOES-10 in the opposite direction; and then after a short interval, the magnetopause moved earthward again and was crossed by GOES-10 at 19:28 UT; at 20:47 UT, the magnetopause

completed last GOES-10 crossing by moving sunward, and the spacecraft returned in the magnetosphere. For the four crossings, GOES-10 was located at MLT of 10:13, 10:30, 10:37, and 11:52, respectively, in time sequence. During the passage of the MCBL, GOES-10 was in the magnetosheath for 77 min (Note that the time scale of the MCBL is 83 min). In the same way, GOES-12 experienced four magnetopause crossing (see Figure 2d; the crossing time is labeled by "A," "B," "D," and "E" respectively): earthward crossing at 19:04 UT, sunward crossing at 19:21 UT, earthward crossing at 19:38 UT and sunward crossing at 20:26 UT. For the four crossings, GOES-12 was located at MLT of 14:14, 14:31, 14:48, and 15:43, respectively, in time sequence. During the passage of the MCBL, GOES-12 was in the magnetosheath for 48 min.

[12] Figure 2 also indicates that the magnetopause crossings via sudden moving was related to strong discontinuities. This is easy to understand since the solar wind dynamic pressure and magnetic field direction are perhaps changed across the discontinuities. The simultaneous crossing of GOES-10 and GOES-12 at 19:21 UT was corresponding to a strong discontinuity labeled by "B" in WIND observations in Figure 2a through which the solar wind dynamic pressure sharply decreased. The crossing of GOES-12 at 19:38 UT was related to a dynamic pressure pulse in strong southward magnetic field (see the vertical line labeled by "D" in WIND observations). The crossing of GOES-12 at 20:26 UT was related to a discontinuity labeled by "E" in WIND observations through which the solar wind dynamic pressure sharply decreased. The crossing of GOES-10 at 20:47 UT was related to a northward turning discontinuity (see the vertical line labeled by "F" in WIND observations). It indicates that the dynamic pressure enhancement and the sustaining southward B_z magnetic field component result in the strong compressional effect of the MCBL. The strong discontinuities lead to the magnetopause crossing at the geosynchronous orbit.

[13] When the MCBL impinged on the magnetosphere, the dayside magnetosphere was strongly compressed to a very small region. In terms of *Shue et al.* [1998] model, the shape and the size of the magnetopause during the passage of the MCBL can be calculated. The closest subsolar standoff distance r_0 is only 5.1 R_E due to the compression, while, on quiet solar wind condition, r_0 is 10–11 R_E. For comparison, Figure 2b presents the shape and location of the magnetopause in terms of *Shue et al.* [1998] model in quiescent condition (green line) and when the subsolar is nearest the Earth during the passage of the MCBL (red line).

3.2. Geomagnetic Storm and Magnetospheric Substorm

[14] As a measure of low-latitude geomagnetic variations, the Sym-H index measures the mean longitudinally symmetric component of the magnetic disturbances, averaged from six globally distributed magnetometers at middle latitudes, and is essentially the same as the hourly Dst index, except that the Sym-H index provides 1-min time resolution. The upper four panels in Figure 3a shows the shifted WIND observations including magnetic intensity and B_z component (in GSM) and solar wind dynamic pressure and the Sym-H index. It can be seen from the Sym-H index that the main phase of an intense geomagnetic storm ($\text{Sym-H}_{\text{min}}$ = −275 nT) was driven during the interval from 19:20 to 21:03 UT, and after a short interval when the magnetosphere entered into the magnetic cloud body, the recovery phase began. This super storm was mainly driven by the intense and long-sustained southward magnetic field inside the magnetic cloud boundary layer.

[15] At about 19:45 UT on 9 November, Polar UVI images (not shown here) showed that a sudden auroral brightening broke up and then the aurora expanded polarward, westward and eastward. These are typical characteristics of auroral substorms. We also examined the simultaneous substorm onset indicators observed by serial LANL satellites, TC-1 and high-latitude geomagnetic stations. Below we will present the identification of this substorm and analyze that the substorm triggering is related to the special magnetic structure of the MCBL.

[16] Serial LANL satellites operate at geosynchronous orbit with continuous particle data in real time acquisition from 1976 to the present. Typically we can receive data from three to five satellites at different MLTs simultaneously. In 2004, the data are available from LANL 1991-080, 1994-084, 97A, 01A, and 02A. During the passage of the MCBL, the five LANL satellites except 1991-080 were located on the nightside at different MLTs. Especially, LANL 02A is near the midnight. Figure 3a presents the particle flux data from LANL 02A during the passage of the MCBL. The corresponding MLTs at which the satellite was located are denoted below the universal time terms. At 19:49 UT, the electron and proton fluxes abruptly increased by one to two orders in less than half minute when 02A was at 00:35 MLT, i.e., dispersionless particle injection was triggered. Twenty minutes min before 19:49 UT, the energetic electron fluxes at all channels and the energetic proton fluxes at higher-energy channels gradually decreased, which corresponds to the substorm expansion phase. After the dispersionless particle injection, the particle fluxes kept higher level until 20:03 UT. This corresponded to the substorm expansion phase. Simultaneously, the LANL 97A satellite at the dawn side and the LANL 01A satellite at the dusk side also observed the similar dispersionless particle injection phenomena (not shown here). The third to sixth panels in Figure 3b show TC-1 observations. The TC-1 spacecraft was at MLT of about 21:50 and 6 R_E from the Earth center during the passage of the MCBL. At 19:53 UT, the tilt angle of the magnetic field abruptly increased by 12°, but 10 min before, it gradually decreased due to the stretching of magnetic field line. Thus we can conclude that magnetic field dipolarization onset was triggered at 19:53 UT. The seventh to tenth panels in Figure 3b present the geomagnetic field observational data from one high-latitude station: DOB. The panels from top to bottom are north (X) and east component (Y) of the horizontal intensity and the vertical component (Z) of the geomagnetic field, as well as Pi2 magnetic pulsation spectrum with period of 40–150 s respectively. The longitude and latitude of DOB stations are 9.11°, 62.07°). When the substorm onset was triggered, DOB was located at evening side at MLT of 22:51. It can be seen that Pi2 pulsation was suddenly enhanced at 19:45 UT. Simultaneously, the negative magnetic bay was triggered, which can be seen from X component of the geomagnetic field in DOB that decrease gradually by ~800 nT.

[17] The aurora breakup, magnetic field dipolarization, dispersionless particle injection, Pi2 pulsation and the polar

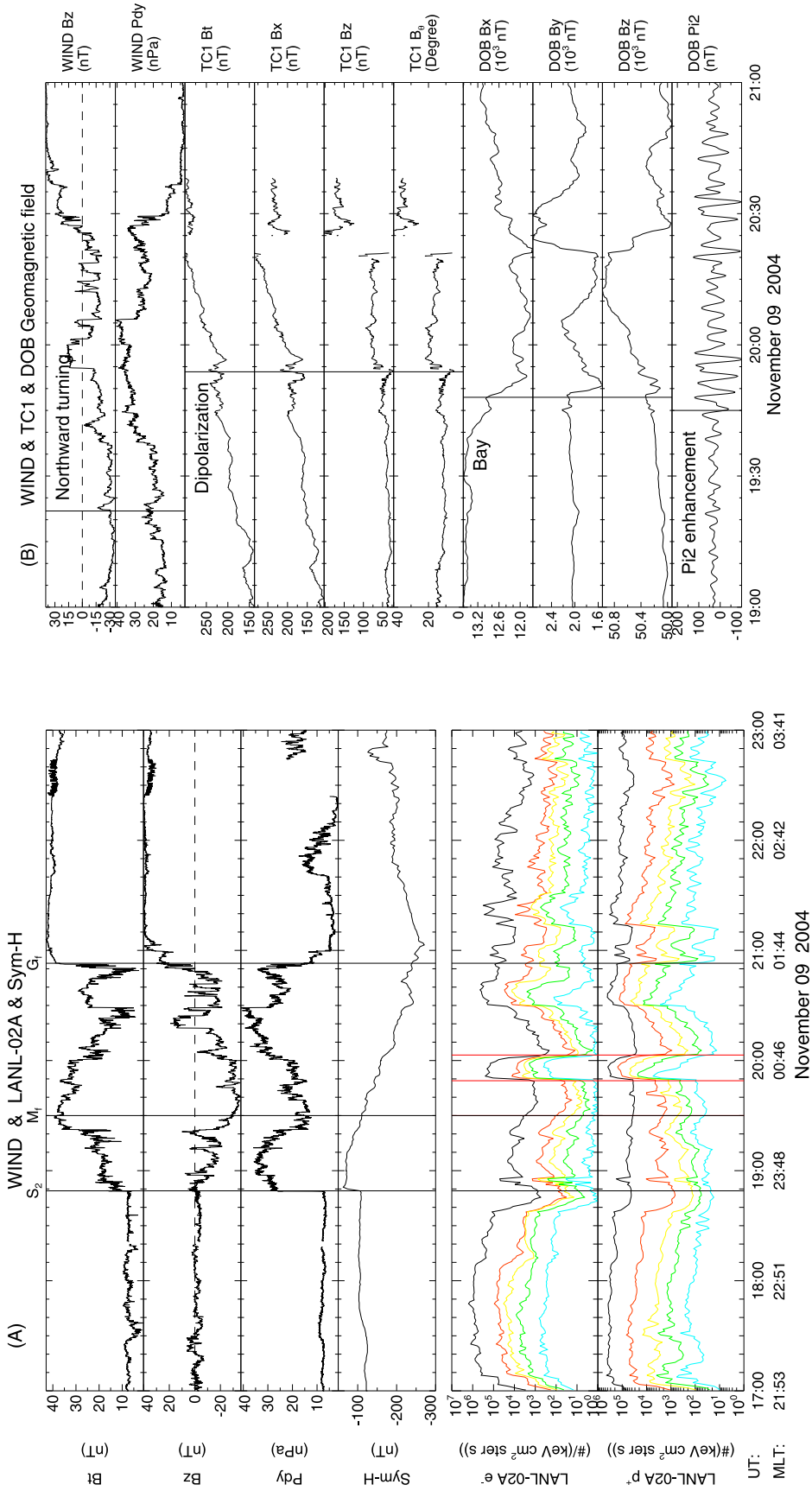

Figure 3. The magnetospheric representations of a typical magnetospheric substorm triggered by the MCBL. (a) LANL 02A dispersionless particle injections; (b) the solar wind trigger, magnetic dipolarization observed by TC-1, as well as the magnetic bay and Pi2 pulsation enhancement observed by high-latitude station DOB.

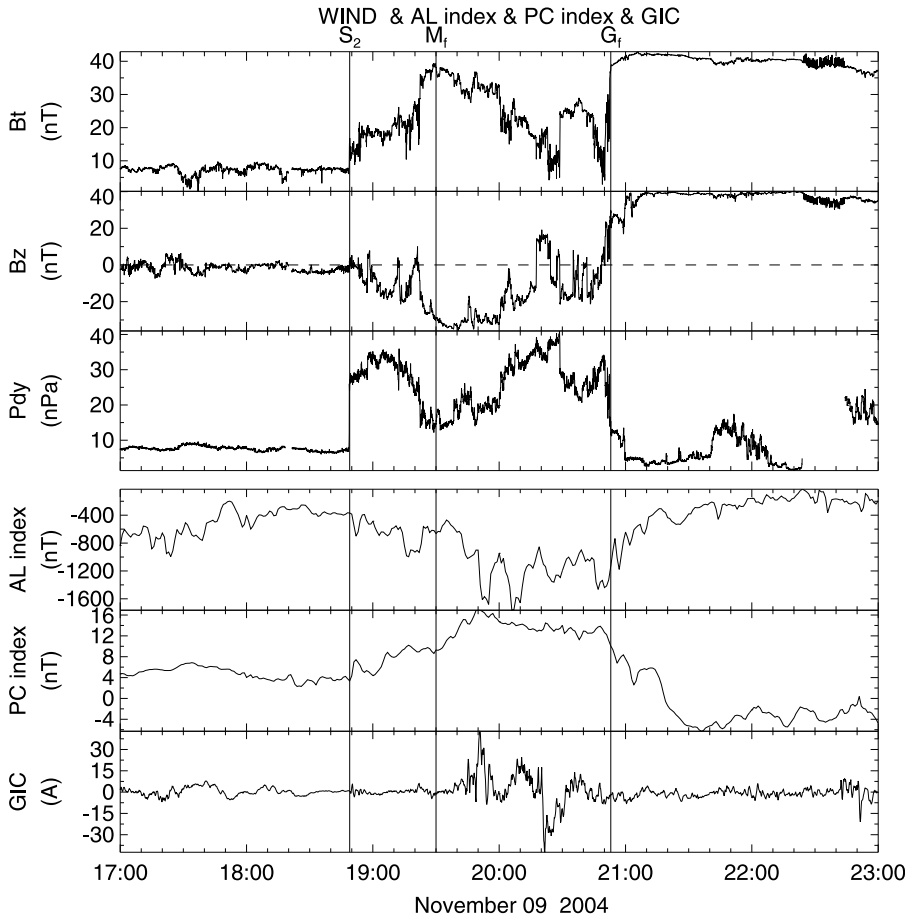

Figure 4. Plot of the GIC data from Mäntsälä, AL index, and PC index during the passage of the MCBL. The solar wind data are shifted by 23 min.

negative bay are all substorm presentations in nightside magnetosphere from different aspects, and give the proxy of substrom onset. Whether the occurrence of substorms is spontaneous or is triggered by abrupt changes of the external solar wind conditions is still a controversial issue. Although there is evidence showing that substorms can occur during stable solar wind and IMF conditions, there is more evidence indicating that substorm occurrences are related to IMF and plasma variations [*Meng and Liou*, 2004]. The large-scale convection electric field in the magnetosphere and the ionosphere are strongly affected by IMF variations: when IMF turns southward or $|B_y|$ increases, the plasma convection electric field is enhanced; on the contrary, when IMF turns northward or $|B_y|$ decreases, the plasma convection electric field is depressed. *Lyons* [1995] proposed that the substorm expansion phase resulted from a reduction in the large-scale electric field imparted to the magnetosphere from the solar wind, after a growth phase when the electric field was enhanced for at least 30 min. Thus it can explain that some substorms are triggered by IMF northward turning after sustaining southward magnetic field for more than 30 min [*Lyons*, 1995, 1996; *Lyons et al.*, 1997]. The top panels in Figure 3b show the magnetic field B_z component and the solar wind dynamic pressure. At 19:00 UT, the direction of IMF turned southward and then kept strong southward (average B_s was 28 nT) for about 21 min. At 19:21 UT, the southward field sharply decreased (i.e., northward turning). Subsequently, the solar wind dynamic pressure was relatively stable. Note that the transit time for the MCBL propagating from the WIND spacecraft to the magnetopause is 23 min. The arrival of the discontinuity with northward turning is just right corresponding to the substorm onset. In terms of Lyons' substorm theory, it can be concluded that during the interval when the MCBL crossed the magnetosphere, the northward turning after sustaining strong southward magnetic field triggered the onset of a typical substrom at 19:45 UT. The substorm triggering is related to the special magnetic structure in the MCBL.

3.3. Geomagnetically Induced Current

[18] Geomagnetically induced current flowing in technological conductor systems such as power grids and pipelines is an end link of the chain of space weather processes from the Sun to the Earth. The GIC flowing in the Finnish natural gas pipeline network have been measured with temporal data resolution of 10 s since November 1998 at Mäntsälä [*Pulkkinen et al.*, 2001; *Viljanen et al.*, 2006a, 2006b; *Pulkkinen et al.*, 2008; *Huttunen et al.*, 2008]. Figure 4 give the GIC measurement at Mäntsälä during the passage of the MCBL with the shifted WIND data, AL index, and PC index also presented. The most intense GIC disturbance is

related to the MCBL passage and in the storm main phase. Associated with the large GIC, the polar ionosphere currents were also strong and disturbed. It can be inferred from the negative magnetic bay structure from the AL index with a maximum of −1764 nT, and the PC index that is a proxy of the polar DP2 current with a maximum of 17 nT. At 20:22 UT, the GIC reached the peak of −42.8 A, which follows the substorm onset. This is the third largest GIC event measured at Mäntsälä since the beginning of continuous observation. *Huttunen et al.* [2008] have found that the MCBL is one of the solar wind drivers of intense GIC event and pointed out that the MCBL can cause large GIC event even if no storm activity takes place. Auroral substorm is one of the major causes of large GIC [*Huttunen et al.*, 2008], and the MCBL is a good candidate driver of the substorm [*Zuo et al.*, 2007], so the MCBL can potentially cause strong GIC disturbances.

4. Summary

[19] As we know, magnetic clouds are very important disturbance source of intense geomagnetic storm and can effectively drive other strong magnetospheric activities. In a broad sense, the magnetic cloud structure (including the ejecta and the driven plasma) consists of three parts that have different magnetic and plasma structures: the sheath region, boundary layer, and the magnetic cloud body. Within the sheath the dynamic pressure is typically high and variable and the magnetic field direction can change for several times from south to north. For the magnetic body the magnetic field direction typically changes smoothly and the dynamic pressure is rather low. While, for the boundary layer, the magnetic field B_z components are more turbulent along with several discontinuities and the dynamic pressure is notably higher when compared to the sheath region and magnetic cloud body.

[20] Although the scale of the MCBL is rather small (half to a few hours for spacecraft passage at 1 AU), it is also a kind of complicated disturbance in interplanetary space from the viewpoint of space weather. In this study, the space weather effects during the passage of one MCBL observed by WIND on 9 November 2004 are intensively investigated. The intense southward magnetic field and very high dynamic pressure within the MCBL make this event quiet exceptional. An intense geomagnetic storm main phase is driven by the sustaining strong southward magnetic field. During the passage of the MCBL, a typical magnetospheric substorm is triggered by northward turning after strong sustaining southward magnetic field inside the MCBL. The substorm onset is synthetically identified by the aurora breakup, magnetic dipolarization, dispersionless particle injection, Pi2 pulsation, and the polar bay. The substorm triggering is related to the special magnetic and plasma structure in the MCBL. The MCBL in company with adjacent sheath region form a dynamic pressure enhancement region, which strongly compressed the magnetosphere and even pushed the magnetopause into the geosynchronous orbit so that two dayside spacecraft GOES-10 and GOES-12 were directly exposed in the magnetosheath. For most of time during the passage of the MCBL, GOES-10, and GOEs-12 were in the magnetosheath. In terms of *Shue et al.* [1998] model, the closest subsolar standoff distance is only 5.1 R_E during the passage of the MCBL. Simultaneously, it can be inferred that the strong dynamic pressure and the strong discontinuities inside the MCBL determine the intense compression effect. The large GIC events receive much concern because strong GIC could damage the normal technological systems such as power transmission lines, long-distance telephone cables, and oil pipelines. *Huttunen et al.* [2008] investigated the solar wind drivers of large GIC during the solar cycle 23 and found the three parts of ICMEs are all effective in causing large GIC. For this concerned MCBL, the very intense GIC was triggered, which is also an evidence to support the result of *Huttunen et al.* [2008].

[21] Similar to this case, majority of MCBLs are dynamic pressure enhancement regions, and there are sustaining southward magnetic field and several strong discontinuities inside these regions, which can potentially lead to global responses in the magnetosphere, on both dayside and nightside. It is significant to further investigate the effects of MCBLs to the magnetosphere-ionosphere coupling system, especially to the ionosphere, and find the commonness to give observational basis for the space weather prediction.

[22] **Acknowledgments.** We acknowledge the use of the data of Wind, GOES, LANL, and the geomagnetic field from the World Data Center (WDC) and of the data of TC-1 supplied by Chinese Double-Star Data Center. The Finnish Meteorological Institute and the Gasum Oy Company are acknowledged for providing the GIC data. This work is jointly supported by the National Natural Science Foundation of China (40804046, 40921063, 40890162, 40674084), 973 program under grant No. 490 2006CB806304, Research Fund for Recipient of Excellent Award of the Chinese Academy of Sciences President's Scholarship, and the Specialized Research Fund for State Key Laboratories.

[23] Zuyin Pu thanks the reviewers for their assistance in evaluating this article.

References

Akasofu, S.-I. (2004), Several 'controversial' issues on substorms, *Space Sci. Rev.*, *113*, 1–40, doi:10.1023/B:SPAC.0000042938.57710.fb.

Borovsky, J. E., and M. H. Denton (2006), Differences between CME-driven storms and CIR-driven storms, *J. Geophys. Res.*, *111*, A07S08, doi:10.1029/2005JA011447.

Burlaga, L. F. (1995), *Interplanetary Magnetohydrodynamics*, New York, Oxford University Press.

Huttunen, K., and H. Koskinen (2004), Importance of post-shock streams and sheath region as drivers of intense magnetospheric storms and high-latitude activity, *Ann. Geophys.*, *22*, 1729–1738.

Huttunen, K. E. J., S. P. Kilpua, A. Pulkkinen, A. Viljanen, and E. Tanskanen (2008), Solar wind drivers of large geomagnetically induced currents during the solar cycle 23, *Space Weather*, *6*, S10002, doi:10.1029/2007SW000374.

Lyon, J. G. (2000), The solar wind-magnetosphere-ionosphere system, *Science*, *288*, 1987–1991, doi:10.1126/science.288.5473.1987.

Lyons, L. R. (1995), A new theory for magnetospheric substorms, *J. Geophys. Res.*, *100*, 19,069–19,082, doi:10.1029/95JA01344.

Lyons, L. R. (1996), Substorms: Fundamental observational features, distinction from other disturbances, and external triggering, *J. Geophys. Res.*, *101*, 13,011–13,026, doi:10.1029/95JA01987.

Lyons, L. R., G. T. Blanchard, J. C. Samson, R. P. Lepping, T. Yamamoto, and T. Moretto (1997), Coordinated observations demonstrating external substorm triggering, *J. Geophys. Res.*, *102*, 27,039–27,052, doi:10.1029/97JA02639.

Meng, C.-I., and K. Liou (2004), Substorm timings and timescales: A new aspect, *Space Sci. Rev.*, *113*, 41–75, doi:10.1023/B:SPAC.0000042939.88548.68.

Pulkkinen, A., A. Viljanen, K. Pajunpaa, and R. Pirjola (2001), Recordings and occurrence of geomagnetically induced currents in the Finnish natural gas pipeline network, *J. Appl. Geophys.*, *48*, 219–231, doi:10.1016/S0926-9851(01)00108-2.

Pulkkinen, A., R. Pirjola, and A. Viljanen (2008), Statistics of extreme geomagnetically induced current events, *Space Weather*, *6*, S07001, doi:10.1029/2008SW000388.

Pulkkinen, T. (2007), Space weather: Terrestrial perspective, *Living Rev. Sol. Phys.*, *4*, 1.

Schwenn, R. (2006), Space weather: The solar perspective, *Living Rev. Sol. Phys.*, *3*, 2.

Sergeev, V. A., R. J. Pellinen, and T. I. Pulkkinen (1996), Steady magnetospheric convection: A review of recent results, *Space Sci. Rev.*, *75*, 551–604, doi:10.1007/BF00833344.

Shue, J.-H., P. Song, C. T. Russell, J. T. Steinberg, J. K. Chao, G. Zastenker, O. L. Vaisberg, S. Kokubun, H. J. Singer, T. R. Detman, and H. Kawano (1998), Magnetopause location under extreme solar wind conditions, *J. Geophys. Res.*, *103*, 17,691–17,700, doi:10.1029/98JA01103.

Viljanen, A., A. Pulkkinen, R. Pirjola, K. Pajunpää, P. Posio, and A. Koistinen (2006a), Recordings of geomagnetically induced currents and a nowcasting service of the Finnish natural gas pipeline system, *Space Weather*, *4*, S10004, doi:10.1029/2006SW000234.

Viljanen, A., E. I. Tanskanen, and A. Pulkkinen (2006b), Relation between substorm characteristics and rapid temporal variations of the ground magnetic field, *Ann. Geophys.*, *24*, 725–733.

Wei, F., R. Liu, Q. Fan, and X. Feng (2003a), Identification of the magnetic cloud boundary layers, *J. Geophys. Res.*, *108*(A6), 1263, doi:10.1029/2002JA009511.

Wei, F., R. Liu, X. Feng, D. Zhong, and F. Yang (2003b), Magnetic structures inside boundary layers of magnetic clouds, *Geophys. Res. Lett.*, *30*(24), 2283, doi:10.1029/2003GL018116.

Wei, F., X. Feng, F. Yang, and D. Zhong (2006), A new non-pressure-balanced structure in interplanetary space: Boundary layers of magnetic clouds, *J. Geophys. Res.*, *111*, A03102, doi:10.1029/2005JA011272.

Zuo, P. B., and X. S. Feng (2007), The plasma and magnetic field characteristics of a double discontinuity in interplanetary space, *Sol. Phys.*, *240*, 347–357, doi:10.1007/s11207-007-0278-7.

Zuo, P. B., F. S. Wei, and X. S. Feng (2006), Observations of an interplanetary slow shock associated with magnetic cloud boundary layer, *Geophys. Res. Lett.*, *33*, L15107, doi:10.1029/2006GL026419.

Zuo, P. B., F. S. Wei, X. S. Feng, and F. Yang (2007), The relationship between the magnetic cloud boundary layer and the substorm expansion phase, *Sol. Phys.*, *242*, 167–185, doi:10.1007/s11207-007-0407-3.

X. S. Feng, W. B. Song, F. S. Wei, X. J. Xu, and P. B. Zuo, SIGMA Weather Group, Center for Space Science and Applied Research, State Key Laboratory of Space Weather, Chinese Academy of Sciences, Beijing 100190, China. (pbzuo@spaceweather.ac.cn)